Evaluation of the mechanical properties of cements with fillers derived from the CO2 reduction of cement plants

Available online at www.sciencedirect.com

ScienceDirect

Procedia Structural Integrity 18 (2019) 472–483

Structural Integrity Procedia

www.elsevier.com/locate/procedia

25th International Conference on Fracture and Structural Integrity

# Evaluation of the mechanical properties of cements with fillers derived from the $CO_2$ reduction of cement plants

I. Cosentino[a], L. Restuccia[a], G. A. Ferro[a]*, F. Liendo[b], F. Deorsola[b], S. Bensaid[b]

[a]*Department of Structural, Construction and Geotechical Engineering (DISEG)-Politecnico di Torino, C.so Duca degli Abruzzi 24, Turin 10129, Italy*

[b]*Department of Applied Science and Technology (DISAT)-Politecnico di Torino, C.so Duca degli Abruzzi 24, Turin 10129, Italy*

**Abstract**

This work introduces a novel method for the development of $CO_2$ recovery systems derived from the production process of cement in order to obtain $CaCO_3$ nanofiller in cement-based composites. Research was carried out in collaboration between the Department of Applied Science and Technology (DISAT) and the Department of Structural, Construction and Geotechnical Engineering (DISEG) of Politecnico di Torino. The objective of this method was dual. Firstly, it aimed to obtain a precipitated calcium carbonate - nano$CaCO_3$ - with a high degree of purity. Secondly, it aimed to optimize the characteristics of these nanoparticles e.g. additional percentages, morphology, particle size distribution or crystal phase, according to their use in cement-based composites. The synthesized nano$CaCO_3$ particles were subsequently added into the cementitious composites in different percentages according to the weight of the cement, in order to understand their behaviour within the cement matrix. The mechanical properties were also evaluated, both at 7 and 28 days, through three point bending and compression tests. The results of the mechanical tests showed a promising improvement in strength and toughness. This study is a first step towards developing a $CO_2$ circular economy.

**Starting date 4 The first day of the month after the signature**


Peer-review under responsibility of the Gruppo Italiano Frattura (IGF) ExCo.

* Corresponding author. Tel.: +39 0110904885;
*E-mail address:* ferro@polito.it

2452-3216 
Peer-review under responsibility of the Gruppo Italiano Frattura (IGF) ExCo.
10.1016/j.prostr.2019.08.189

*Keywords:* carbon dioxide; nanoCaCO$_3$; calcite; cementitious composites; mechanical properties; flexural strength; compressive strength; fracture energy.

## 1. Introduction

The cement industry has a significant role in the emission of carbon dioxide, equivalent to about 7% of total world $CO_2$ production (Oh et al., 2014). Cement production generally emits 0.65 – 0.95 tonne $CO_2$ per tonne cement[1]. Although cement contribution in concrete is merely 20% of the total volume, it is responsible for approximately 90% of the total emission of $CO_2$ (Yang et al., 2015) and the majority of this emission is due to the heating of limestone during the calcination process.

For this reason, in recent years, concrete technology is increasingly relying on "green chemistry", through the study of new materials which can decrease and/or replace the amount of cement in the production of concrete.

Different waste materials are being added to cementitious materials to improve their mechanical properties and to reduce the impact of greenhouse gases. Pyrolysis represents a promising approach to convert organic waste into biochar, a porous carbonaceous solid material which can be used as nano/micro filler in cement-based composites.

A standardized biochar, provided by UK Biochar Centre, was investigated as a nano filler in cement-based composites at Politecnico di Torino, ensuring the reproducibility of cement mixtures (Cosentino, 2017). Although, in terms of flexural strength and fracture energy, results were inferior compared to the previous studies conducted at Politecnico di Torino (Restuccia, 2016) where self-produced pyrolyzed agro-food waste was used for high-performance sustainable cementitious composites. Nonetheless, an overall enhancement of mechanical properties was recorded with the introduction of the standardized biochar in cementitious composites. Some parameters of biochar processes, e.g. production, temperature, heating rate or pressure, as well as some biochar features such as carbon content, particle size distribution or porosity dramatically influence the enhancement of mechanical properties of cementitious composites (Cosentino et al, 2018). Although the parameters are not optimal, biochar can be used to create new green building materials because of its effectiveness in cementitious composites.

Restuccia and Ferro, 2016 used two types of pyrolyzed agro-food waste, coffee powder and hazelnut shells, as carbon nano-aggregates, in different percentages of addition according to the cement weight. Results demonstrated that small amounts of pyrolyzed materials improved mechanical properties of cementitious composites, as they can increase the flexural and compressive strength, and also the fracture energy with a more tortuous crack path which increases the final fracture surface.

Carbon nano/micro particles obtained by controlled pyrolysis of peanut (PS) and hazelnut (HS) shells were used in the production of high-performance cement composites. When added to cement paste, up to 1 wt%, these materials led to an increase of the cement matrix flexural strength and of toughness. Furthermore, an enhancement in shielding effectiveness was observed. In the case of PS addition, the percentage of particles which ensured maximum shielding effectiveness also coincided with maximum value of fracture energy, making it possible to prepare cementitious materials optimized both from a mechanical and an electromagnetic shielding point of view (Khushnood,2016).

Micro-carbonized particles were prepared from hemp hurd (HH) by controlled pyrolysis. The analysis of flexural strength values showed a mixed trend of increase and decrease in proportion to variations of the content of carbonized particles addition. A slight increase of 7% in the modulus of rupture was achieved by adding 0.08 wt% HH, while a noticeable decrease occurred on further additions up to 3%. Evaluated toughness indices of cement composites demonstrated that the addition of HH significantly increased the fracture toughness. It is believed that the presence of a high number of irregular-shaped carbonized particles influences the crack paths by increasing their tortuosity. The maximum compressive strength enhancement was about 58% at 1 wt% inclusion, which can be related to the filling action of inert particles in the cement matrix (Ferro et al, 2014).

[1] Global CCS Institute, Global Status of CCS 2016.

Innovative cementitious composites with carbon-based pyrolyzed micro-aggregates were tested until complete fracture. Images of the crack paths across the tested specimens were acquired by scanning electron microscopy and their fractal dimension was calculated via the box counting method. Results showed that the pyrolyzed micro-aggregates, characterized by high strength and stiffness due to their significant carbon quantity, can alter the crack path by increasing its tortuosity, thus inducing toughening mechanisms in the cementitious composites. This favourable behaviour was explained by means of fractal geometry: it is found that, the greater the fractal dimension of the crack path, the higher the fracture energy (Restuccia et al, 2017).

Since the invention of nanomaterials, concrete technology has made significant progress in exploring the effects of nanomaterials in cementitious composites and their potential applications. Many nano-additives generate superior results to those of their micro counterparts.

Pyrolyzed hazelnut shells, already experimented as nanofiller in previous studies (Restuccia, 2016), were used with an order of magnitude greater in terms of the particle size distribution (some micron up to 140 μm). Three-point bending and compression tests results revealed that it is possible to use pyrolyzed materials with coarser particle size, ensuring the improvement of mechanical properties in terms of flexural and compressive strength, but not in terms of ductility, which is only obtained when using smaller particles (Restuccia et al, 2018).

Nanomaterials can enhance performance of cement-based material given their physical effect (filling and nucleation effects) as well as their chemical reactivity (Sanchez et al., 2010). Nano-silica (nano-$SiO_2$) (Ji, 2005), nano-alumina (nano- $Al_2O_3$) (Li, Wang et al, 2006), nano-titanium oxide (nano-$TiO_2$) (Li, Zhang et al., 2007), nano-$CaCO_3$ (Shaikh et al., 2014), nano iron ($Fe_2O_3$), and nanotubes (Metaxa et al., 2009) have been studied for use in cement-based materials.

This study presents for the first time the design and optimization of the $CaCO_3$ nanofiller production process by $CO_2$ recovery derived from cement manufacturing. Recycling of carbon dioxide in the cement industry can produce added-value additives that can be used to improve the quality of cement (cement additives, nano-fillers for concrete). It could also reduce the energy intensity of cement production (grinding aids, accelerators) and promote an effective purification of $CO_2$ from combustion gases (ionic liquids integrated with amines). All of these constitute a step towards a $CO_2$ circular economy.

Although $CaCO_3$ was first considered as a filler, some studies indicate that it reacts chemically, accelerates the cement hydration process, and in turn, increases the early-age strength of conventional cementitious materials, because of the additional quantity of C-S-H gel produced (Liu et al, 2012) (Sekkal et al., 2017).

Calcium Carbonate nanoParticles (CCnP) are synthesized via a carbonation route (Declet, 2016; Kawano, 2009) and have a large range of applications. Since their characteristics, such as size and morphology, are easily tunable through the synthesis method (Declet, 2016) (Ding, 2018) (Ulkeryildiz, 2016). They are widely used as filler materials and, because of their porosity, non-toxicity and biocompatibility, they are also used in the biomedical and food industry (Maier, 2008).

The effects of the operating conditions on the morphology and growth rate of calcium carbonate in a gas-liquid-solid reactive crystallizer have been widely studied (Sun, 2011) (Ding, 2018). Sun et al. (2011) synthesized calcium carbonate nanoparticles with a rhombohedral morphology in a rotating packed bed. They concluded that high turbulent conditions led to obtain smaller particles. Ding and co-workers (2018) obtained different polymorph and morphologies: needle-like aragonite particles, cubic calcite particles and spherical vaterite particles. Several process variables have been investigated, including the pH of the solution, the concentration of the calcium ion, the concentration ratio of $[HCO_3]$ / $[CO_2]$ (Chen, 1997) (Ulkeryildiz, 2016), and the gas liquid mixing mode (Sun, 2011). The last variable is important, since macro and micromixing occur simultaneously in the reactors and play an important role on reactive precipitation. Macro refers to a uniform spatial concentration distribution on the vessel scale, while the distribution on the molecular scale is reached by an intense micromixing (Chang, 2003). A uniform spatial concentration distribution on the molecular scale provides the same treatment process for each molecule. Thus, a homogeneous product with a narrow particle size distribution. Hence, the $CO_2$ absorption mechanism plays a crucial role in the $CaCO_3$ particle synthesis in order to obtain a high micromixing level. Micromixing is a key factor determining the degree of the supersaturation concentration of the solute and its local spatial distribution (Sun, 2011).

Once the $CO_2$ is absorbed, the $CaCO_3$ precipitation takes place and its driving force is supersaturation, determined by the product of the ionic concentration of calcium and carbonate ions. Precipitation involves four steps: (i)

dissolution of CaO, (ii) mass transfer between the $CO_2$ phase and the water phase and the formation of carbonate ions, (iii) a chemical reaction, and (iv) crystal growth which results in higher absorption rates in water compared to other similar compounds. In fact, they do not occur in this specific order but simultaneously, therefore it is important to control these three steps during precipitation. The $CO_2$ absorption step is crucial, and it is important to control it.

Different reactor configurations have been studied for the synthesis of calcium carbonate via carbonation (Chilakala Ramakrishna, 2017). Both a stirred tank reactor with different bubble generators and a rotating bed reactor have been tested in order to perform the $CaCO_3$ nanoparticles synthesis (Chen, 1997) (Sun, 2011) (Ulkeryildiz, 2016).

In this study, a packed bed reactor is proposed to obtain $CaCO_3$ nanoparticles via carbonation. This apparatus can provide a good mixing gas-liquid and control the $CO_2$ absorption step. The particles obtained through this method were tested following a standard European procedure to determine their effect as a cement filler.

Carbon capture and storage has a unique role to play in achieving critical emissions reductions for the cement industry. To the best of our knowledge, this is the first study to develop $CO_2$ recovery systems derived from the production process of cement in order to obtain $CaCO_3$ nanofiller in cement-based composites.

## 2. Materials and methods

### *2.1. Materials*

Ordinary Portland Cement, CEN Standard sand, deionized water and Calcium Carbonate nanoParticles were used for the preparation of cement mortars. Cement (i.tech ULTRACEM 52,5 R) was provided by HEIDELBERGCEMENT Group. It is characterized by the rapid development of the initial resistance and it contains, according to the composition of the European Standard EN 197-1 (referring to the mass of the cement excluding calcium sulphate and additives), 95% ÷ 100% clinker, while the remaining part is consisting of any secondary constituents. CEN Standard sand is pre-packed in bags with a content of (1350 ± 5) g and the contents of each bag complies with the particle size distribution specified in Table 1 as determined by sieve analysis on a representative sample of sand of total mass not less than 1345 g, according to the European Standard EN 196-1.

Table 1. Particle size distribution of the CEN Reference Sand.

| Sieve analysis | | | | | | | |
|---|---|---|---|---|---|---|---|
| Square mesh size | mm | 2.00 | 1.60 | 1.00 | 0.50 | 0.16 | 0.08 |
| Cumulative sieve residue | % | 0 | 7 ± 5 | 33± 5 | 67 ± 5 | 87 ± 5 | 99 ± 1 |

In the $CaCO_3$ synthesis, a slurry prepared with an analytical grade of CaO (Merck, purity ≥ 99%) and deionized water, and $CO_2$ (purity: 99.9%, supplied from SIAD, Italy) were employed.

The synthetized $CaCO_3$ nanoparticles were incorporated in the cement mortars with different additional percentages according to the weight of cement (2% wt and 3% wt).

### *2.2. Methods*

#### *2.2.1. Synthesis of $CaCO_3$ particles*

The $CaCO_3$ particles were synthesized through a carbonation route in packed bed reactor. This reactor was constructed from a light polyvinyl chloride (PVC) pipe and filled with <10 mm industrial produced monolith. Reactor and packing parameters are summarized in the Table 2. The synthesis was carried out at continuous conditions, starting from a CaO slurry (0.015 M) in an experimental setup as shown in Figure 1. The slurry and the gas stream were flowed to the bottom of the PBR, where contacted in a T-mixer. The precipitated particles were rapidly filtered by vacuum and dried at 60 °C overnight.

Table 2. Specifications of the PBR employed in the synthesis of $CaCO_3$.

| Specifications of the PRB | Units | Values |
|---|---|---|
| Volume of the PBR, $V_R$ | $m^3$ | $2.36 \times 10^{-6}$ |
| Radius of the packing, $r_p$ | m | 2 |
| Axial length of the packing, $L_p$ | m | 4 |
| Surface area of the dry packing per unit volume of the PBR, $a_p$ | $m^2/m^3$ | 600 |
| Voidage of the dry packing | $m^3/m^3$ | 0.55 |

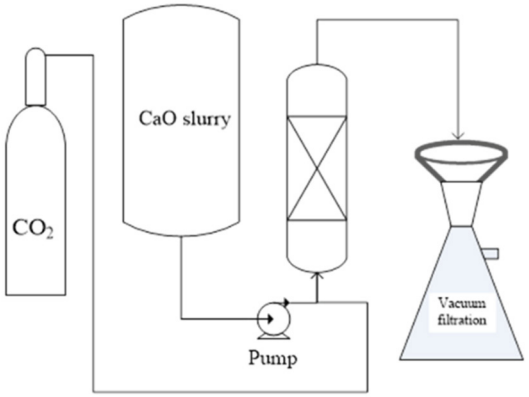


Figure 1. Experimental setup for $CaCO_3$ particles synthesis.

### *2.2.2. Characterization of $CaCO_3$ particles*

Different characterization analysis was performed on the $CaCO_3$ powder. The dried powder was re-dispersed in isopropanol (1g/L) and about 1 mL of sample was put into a UV cuvette and size and size distribution were measured by dynamic light scattering (DLS) method using particle size analyzer (Malvern nano ZS model). A 1 mL was also introduced into a zeta cell, and zeta potential values were measured by the Malvern Zeta Sizer.

The phase purity of the samples was examined by X-ray diffraction in the 2θ range of 20-70° with a scanning step of 0.013° and a radiation CuKα, k = 1.54056 Å. Morphological characterization was obtained using scanning and transmission electron microscopy (ZEISS MERLIN FE-SEM operated at 3 kV). The samples were prepared for electron microscopy observations by suspending a small amount of nanoparticles in isopropanol, through ultrasonic mixing for 30 min, and subsequently by placing a drop of the dispersion on a copper grid coated with a layer of amorphous carbon. Surface area was determined from $N_2$ adsorption and desorption isotherms, measured at the temperature of liquid $N_2$ (Quantachrome Autosorb-1). The surface area was calculated from the Brunauer-Emmet-Teller (BET) equations. All samples were outgassed at 120 °C overnight prior to measurement.

### *2.2.3. Preparation of experimental specimens*

The preparation of cement mortars was made according to the European Standard EN 196-1 “Methods of testing cement - Part 1: Determination of strength”. The proportions by mass are one part of the cement, three parts of CEN Standard sand and one half part of water (water/cement ratio 0.50). Each batch for three test specimens consists of 450 g of cement, 1350 g of sand and 225 g of water; and Calcium Carbonate nanoParticles were added in different percentages (2%; 3%) according to the weight of cement in a solution with deionized water (Table 3).

Table 3. Cement Mortars Mixtures.

| ID Mixture | Cement | Water | w/c ratio | Standard CEN Sand | Calcium Carbonate | |
|---|---|---|---|---|---|---|
| | [g] | [g] | [-] | [g] | [g] | [%] |
| Mortar | 450 | 225 | 0.5 | 1350 | 0 | 0 |
| Mortar_$CaCO_3$_2% | 450 | 225 | 0.5 | 1350 | 9.0 | 2 |
| Mortar_$CaCO_3$_2%_ub | 450 | 225 | 0.5 | 1350 | 9.0 | 2 |
| Mortar_$CaCO_3$_3%_ub | 450 | 225 | 0.5 | 1350 | 13.5 | 3 |

The solution was also subjected to ultrasonic bath for 8 minutes to promote a better dispersion of particles. The cement mortar was mixed in a stainless-steel bowl by means a stainless-steel blade in a planetary movement around the axis of the bowl at controlled speeds by an electric motor. The cement and the solution of deionized water with calcium carbonate were placed into the bowl, taking care to avoid loss of liquid solution or cement powder. Immediately the liquid and the cement were brought into contact, the mixer started at low speed. After 30 s of mixing, the sand was added during the next 30 s. Then the mixer switched to the high speed and continued for an additional 30 s. The mixer was stopped for 90 s, removing the mortar adhering to the wall of the bowl. The mixing continued at the high speed for 60 s. (Figure 2) The test specimens (40 mm x 40 mm x 160 mm) were made by introducing the first of two layers of mortar into each of the mould compartments, directly from the mixing bowl and then compacted using 60 jolts of the jolting apparatus. The second layer was introduced and compacted with a further 60 jolts. Specimens were stored in a humid atmosphere for at least 24 hours and, once the specimens were unpacked, they were submerged in water at (20.0 ±1.0) ° C for 7 and 28 days curing (European Standard EN 196-1).


Figure 2. Preparation cement mortar mixtures

## 3. Mechanical test activity

Each experimental specimen was subjected to Three Point Bending test by using a Zwick Line-Z050 machine with a load cell of 50 kN. The load was applied vertically by means of the loading roller and was increased at the rate of 50 N/s until fracture. The distance between the supports was fixed to 100 mm (Figure 3).
Flexural strength, $R_f$, in megapascals, has been calculated as it follows (European Standard EN 196-1):

$$R_f = \frac{1.5 * F_t * l}{b^3} \quad [MPa] \tag{1}$$

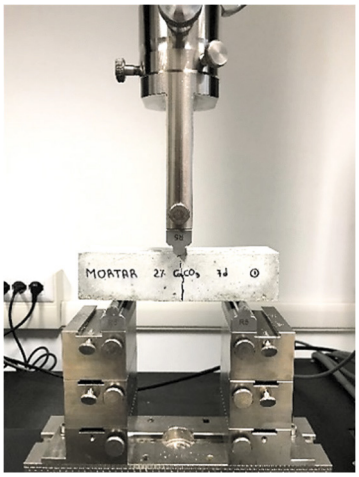


Figure 3. TPB test until experimental specimen fracture

in which $F_t$ represents the load applied to the middle of the prism at fracture, in newtons; $l$ is the distance between the supports, in millimeters; $b$ is the side of the square section of the prism, in millimeters.

Compression test was carried out on halves of the prism broken either as described in TPB test by using Zwick Roell SMART PRO testing machine with a load cell of 1000 kN. The load was applied vertically by the platens of the machine, centering the prism halves laterally to the platens within ± 0.5 mm and longitudinally such that the end face of the prism overhangs the platens by about 10 mm. The load was increased at the rate of 2400 N/s over the entire load application until fracture.

Compressive strength, $R_c$, in megapascals, has been calculated as it follows (European Standard EN 196-1):

$$R_c = F_C/A \ [MPa] \tag{2}$$

in which $F_c$ represents the maximum load at fracture, in newtons; $A$ is the area of the platens in square millimetres.

## 4. Results and discussion

The synthesized $CaCO_3$ phase purity was characterized by XRD pattern, shown in Figure 4.
The diffraction peaks are well consistent with pure calcite pattern, which is the most stable $CaCO_3$ crystalline phase (Chen, 1997) (Rodriguez-Blanco, 2011; Nehrke, 2007; Kawano, 2009). The sharpness of these peaks indicates the highly crystalline nature of the material. No presence of other $CaCO_3$ crystalline phase, such as aragonite and vaterite, was determined.

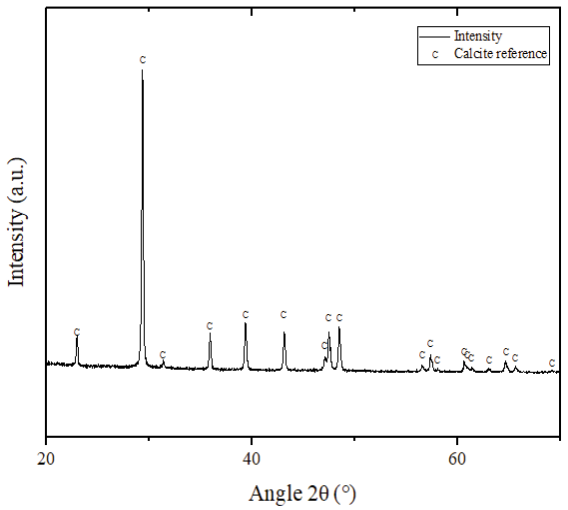


Figure 4. XRD spectra of $CaCO_3$ particles.

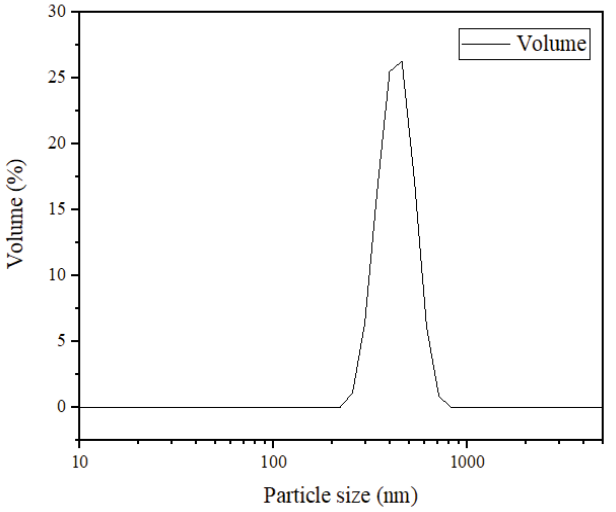


Figure 5. Particle size distribution of $CaCO_3$ powder.

Figure 5 shows a narrow PSD, which is not in a good agreement with the FESEM micrographs (Figure 6), where nanosized cubic calcite primary particles and varied shape nanoaggregates can be observed. These nanoaggregates are formed by cubic particles, which is the classical morphology of calcite crystals (Chen, 1997) (Declet, 2016). Regarding to the specific surface area, since mean diameter of the particles was about 600 nm, but they have a form of aggregate consisting of nano-sized particles. Thus, the $CaCO_3$ powder was expected to have a large specific surface area just as large as 5 $m^2/g$ due to unique structure of secondary aggregated particles.

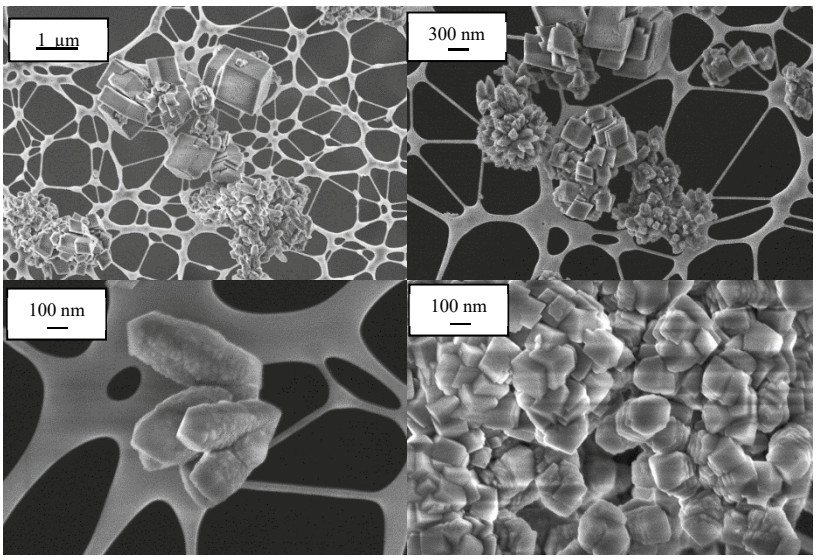


Figure 6. FESEM micrographs of $CaCO_3$ particles.

The flexural strength test results were calculated as the arithmetic mean of the three individual results obtained from a determination made on a set of three prisms. The compressive strength test results were calculated as the arithmetic mean of the six individual results obtained from the six determinations made on a set of three prisms, according to the European Standard EN 196-1. The mean value of maximum force, flexural and compressive strength were calculated both at 7 and at 28 days for all the cement mortar mixtures (Figures 7-8).

The experimental specimens characterized by the addition of 2% of $CaCO_3$ showed good mechanical properties only if the ultrasonic bath for water and nanoparticles was included during the preparation of the mortar. The results showed that the mean value of the maximum force, the flexural and the compressive strength increased (by 10%) in these experimental specimens with respect to sample mortars, but this rise was observed only at 7 days. At 28 days, the mechanical properties decreased in the cement mixtures with calcium carbonate nanoparticles incorporated.

On the other hand, the cement mortars prepared without the utilization of the ultrasonic bath gave bad results both at 7 and 28 days. Thus, the ultrasonic bath is necessary to promote the dispersion of the nanoparticles in the deionized water and in cement matrix.

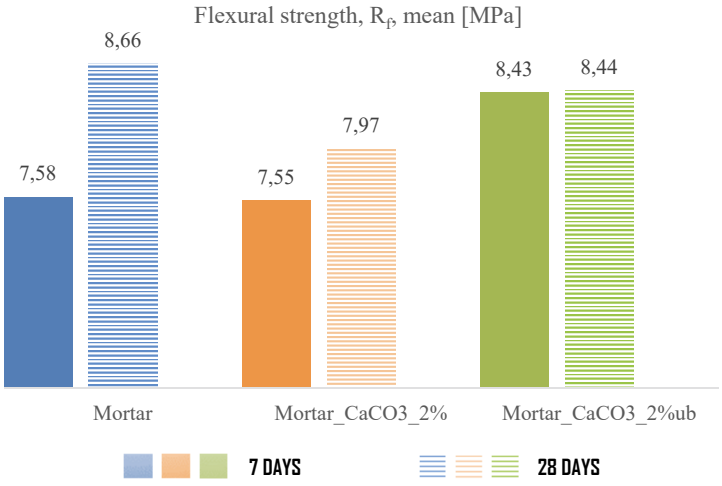


Figure 7: Flexural strength (mean value) after 7-28 days curing.

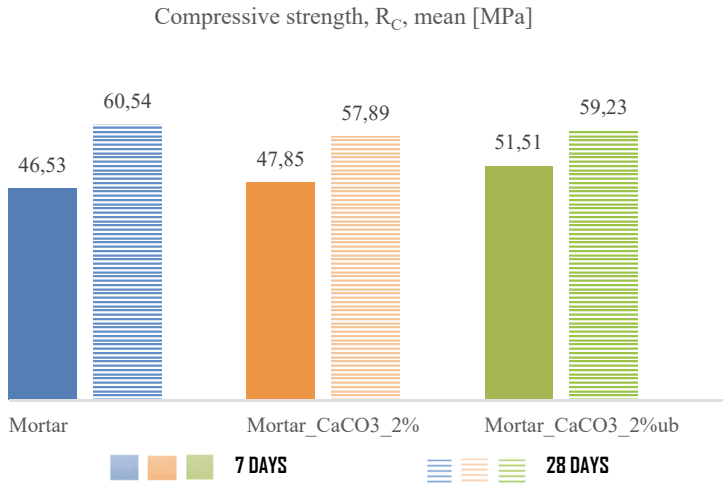


Figure 8: Compressive strength (mean value) after 7-28 days curing.

The experimental campaign also envisaged incorporating a quantity equal to 3% of nanoCaCO$_3$ in cement mortars, by evaluating the flexural and compression tests results. (Figure 9 e 10). However, the 2% addition of nanoCaCO$_3$ proved to be the optimal additional percentage into cement mortars.

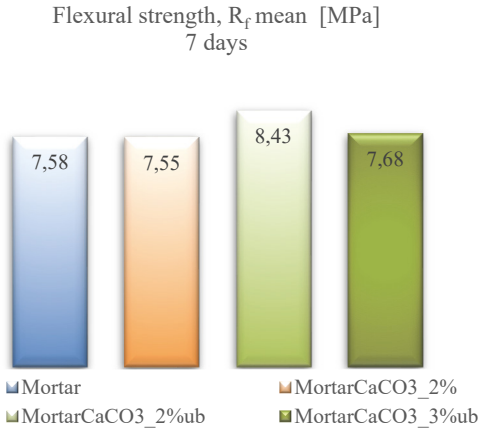


Figure 9: Flexural strength (mean value) after 7 days curing.

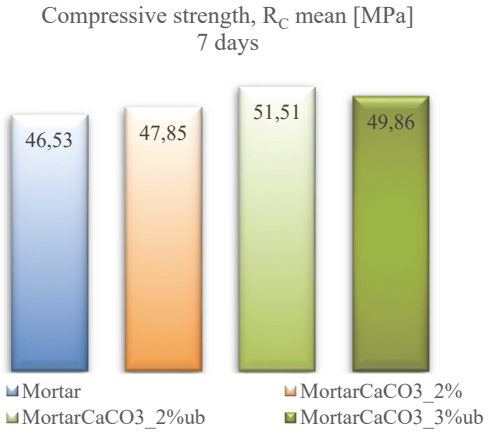


Figure 10: Compressive strength (mean value) after 7 days curing.

From Load-Displacement curves obtained from the TPB and compression tests it was possible to calculate the mean value of the elastic modulus, that represents the slope in σ-ε curves graph. It increased with the additional percentages of CaCO$_3$ equal to 2% and 3% compared to sample mortars only at 7 days (respectively by 29% and 26% in flexural tests and respectively by 11% and 9% in compression tests) as shown in Figures 11a and 12a. At 28 days, there were no improvements to test results for the elastic modulus at 28 days by incorporating calcium carbonate nanoparticles (Figure 11b -12b).

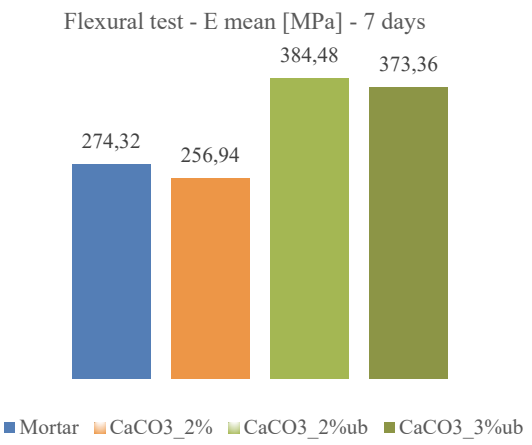


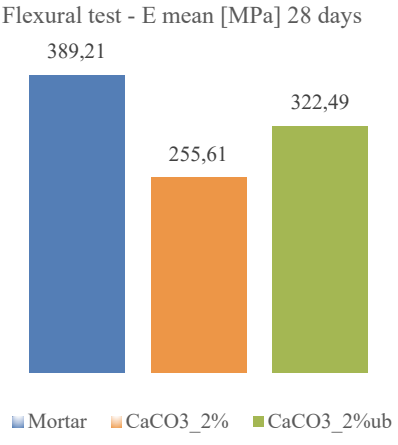


Figure 11: Flexural test: a) Elastic Modulus (mean value) after 7 days curing - b) Elastic Modulus (mean value) after 28 days curing.

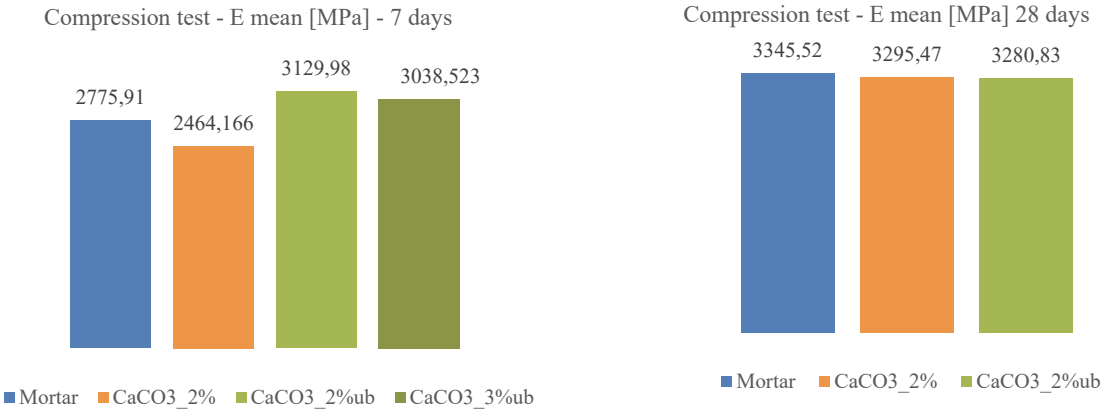


Figure 12: Compression test: a) Elastic Modulus (mean value) after 7 days curing - b) Elastic Modulus (mean value) after 28 days curing.

## 5. Conclusions

One ton of cement production causes 0.95 t of $CO_2$ (Ludwig and Zhang, 2015). This has a serious environmental and economic impact. This study showed that $CO_2$ can be recycled in the cement industry producing added-value additives that can be used to improve the quality of cement.
This work investigated the effects of incorporating precipitated calcium carbonate with a high degree of purity by $CO_2$ recovery derived from cement manufacturing. The design and optimization of the production process of the $CaCO_3$ nanofillers were carried out. By employing a packed bed reactor, nanosized pure calcite particles were obtained via a carbonation route. The synthesized nano$CaCO_3$ particles were added into the cement mortars in different percentages (2%; 3%) according to the weight of the cement, in order to understand their behaviour within the cement matrix. The mechanical properties were evaluated, both at 7 and 28 days, through three point bending and compression tests. Results showed that the mean value of the flexural strength, the compressive strength and the elastic modulus were increased by up to 11%, 11% and 29 %, respectively, after 7 days curing. The optimal additional percentage of nano$CaCO_3$ filler into cement mortars was 2%, when using an ultrasonic bath to disperse nanoparticles in deionized water, thus avoiding their agglomeration. To sum up, $CaCO_3$ increases the early-age strength of conventional cementitious materials, but the experimental campaign suggested that, at 28 days, a decrease of mechanical properties occurred in experimental specimens characterized by the addition of calcium carbonate compared to sample mortars. The results of the present investigation constitute a first step towards achieving a $CO_2$ circular economy.

## 6. Acknowledgements

This project has received funding from the European Union's Horizon 2020 research and innovation program under Grant Agreement number 768583– RECODE (Recycling carbon dioxide in the cement industry to produce added-value additives: a step towards a $CO_2$ circular economy) project (https://www.recodeh2020.eu/).

## 7. References

Ataki, A., Bart, H.J., 2004. The use of the VOF-model to study the wetting of solid surfaces. Chem. Eng. Technol., 1109-1114.
Ataki, A., Bart, H.J., 2006. Experimental and CFD simulation study for the wetting of a structured packing element with liquids. Chem. Eng. Technol., 363-347.
Chen, J.F., Shao, L., 2003. Mass production of nanoparticles by high gravity reactive. China Particuol, 1, 64-69.
Cosentino, I., 2017. The use of Bio-char for sustainable and durable concrete. Master Thesis, Politecnico di Torino.

Cosentino, I., Restuccia, L., Ferro, G.A., Tulliani, J.M., 2018. Influence of pyrolysis parameters on the efficiency of the biochar as nanoparticles into cement-based composites. Procedia Structural Integrity 13, 2132-2136.

David, R., 2001. General rules for prediction of the intensity of micromixing effects on precipitations. Powder Technology, 2-8.

Declet, A., Reyes, E., 2016. Calcium carbonate precipitation: a review of the carbonate crystallization process and applications in bioinspired composites. Adv. Mater. Sci. 44, 87-107.

European Standard EN 197-1, 2006. Cement - Part 1: Composition, specifications and conformity criteria for common cements.

European Standard EN 196-1, 2007. Methods of testing cement - Part 1: Determination of strength.

Ferro, G.A., Ahmad, S., Khushnood, R.A., Restuccia, L., Tulliani, J.M., 2014. Improvements in self-consolidating cementitious composites by using micro carbonized aggregates. Frattura ed Integrità Strutturale 30, 75-83.

Kawano, J., Shimobayashi, N., 2009. Precipitation diagram of calcium carbonate polymorphs: its construction and significance. J. Phys. Condens. Matter, 21.

Ji, T., 2005. Preliminary study on the water permeability and microstructure of concrete incorporating nano-$SiO_2$. Cem. Concr. Res. 35 (10) 1943e1947.

Khushnood, R.A., Ahmad, S., Restuccia, L., Jagdale, P., Spoto, C., Tulliani, J.-M., Ferro, G.A., 2016. Carbonized nano/microparticles for enhanced mechanical properties and electromagnetic interference shielding of cementitious materials. Frontiers of Structural and Civil Engineering 10 (2), 209-213.

Liu, X., Chen, L., Liu, A., Wang, X., 2012. Effect of Nano-$CaCO_3$ on Properties of Cement Paste. Energy Procedia 16, 991 – 996

Li, Z.H., Wang, H.F., He, S., Lu, Y., Wang, M., 2006. Investigations on the preparation and mechanical properties of the nano-alumina reinforced cement composite. Mater. Lett. 60 (3), 356-359.

Li, H., Zhang, M.H., Ou, J.P., 2007. Flexural fatigue performance of concrete containing nano-particles for pavement, Int. J. Fatigue 29 (7) 1292e1301.

Maier, C., Calafut, T., 1998. Fillers and reinforcements. In Polypropylene (p. 49-56).

Metaxa, Z.S., Konsta-Gdoutos, M.S., Shah, S.P., 2009. Carbon nanotubes reinforced concrete. ACI Spec. Publ. 267, 11e20.

Murugesan, T., Sivakumar V., 2002. Pressure Drop and flow regimes in cocurrent gas-liquid upflow through packed beds. Chemical Engineering Journal, 88, 233-243.

Nehrke, G., Van Cappellen, P., 2006. Framboidal vaterite aggregates and their transformation into calcite: a morphological study. Journal of crystal growth 287,2, 528-530.

Oh, D.-Y., Noguchi, T., Kitagaki, R., Park, W.-J., 2014. $CO_2$ emission reduction by reuse of building material waste in the Japanese cement industry. Renew. Sust. Energ. Rev. 38:796-810.

Chen, P.C., Clifford, Y., Lee, K.C., 1997. Morphology and growth rate of calcium carbonate crystals in a gas-liquid-solid reactive crystallizer. Chemical Engineering Science, 4171-4177.

Restuccia, L., Ferro, G.A., 2016. Promising low-cost carbon-based materials to improve strength and toughness in cement composites. Construction and Building Materials 126, 1034–1043.

Restuccia, L., Ferro, G.A., 2018. Influence of filler size on the mechanical properties of cement-based composites. Fatigue and Fracture of Engineering Materials and Structures 41 (4), 797-805.

Restuccia, L., 2016. Re-think, Re-use: agro-food and C&D waste for high-performance sustainable cementitious composites. Ph.D. Thesis, Politecnico di Torino.

Restuccia, L., Reggio, A., Ferro, G.A., Kamranirad, R., 2017. Fractal analysis of crack paths into innovative carbon-based cementitious composites. Theoretical and Applied Fracture Mechanics 90, 133-141.

Ramakrishna, C., Thenepalli, T., Ahn, J.W., 2017. Evaluation of various synthesis methods for calcite-precipitated calcium carbonate (PCC) formation. Korean Chem. Eng. Res., 279-286.

Rodriguez-Blanco, J.R., Shaw, S., Benning, L.G., 2011. The kinetics and mechanisms of amorphous calcium carbonate (ACC). Nanoscale, 265-271.

Sanchez, F., Sobolev, K., 2010. Nanotechnology in concrete e a review, Constr. Build. Mater. 24 (11) 2060e2071.

Shaikh, F.U.A., Supit, S.W.M., 2014. Mechanical and durability properties of high volume fly ash (HVFA) concrete containing calcium carbonate ($CaCO_3$) nanoparticles. Constr. Build. Mater. 70, 309-321.

Sekkal, W., Zaoui, A., 2017. Enhancing the interfacial bond strength of cement nanocomposite with carbonate nanostructure. Composites Part B 124, 111e119.

Sun, B.C., Wang, X.M., Chen, J.M., Chu, G.W., Chen, J.F., Shao, L., 2011. Synthesis of nano-$CaCO_3$ by simultaneous absorption of $CO_2$ and $NH_3$ into $CaCl_2$ solution in a rotating packed bed. Chemical Engineering Journal, 731–736.

Ulkeryildiz, E., Kilic, S., 2016. Nano-$CaCO_3$ synthesis by jet flow. Colloids and Surfaces A: Physicochemical and Engineering Aspects, 34-40.

Ding, Y., Y. L.-Y. 2018. Controllable synthesis of all the anhydrous $CaCO_3$ polymorphs with various morphologies in $CaCl_2$-$NH_3$-$CO_2$ aqueous system. Powder Technology, 410-420.

Yang, K.H., Jung, Y.B., Cho, M.S., Tae, S.H., 2015. Effect of supplementary cementitious materials on reduction of $CO_2$ emissions from concrete. J. Clean. Prod. 103:774-783.